Research article

A new CO_2 refrigeration system with two-phase ejector and parallel compression for supermarkets

Bourhan Tashtoush [a,*], Haythem Sahli [b], Mouna Elakhdar [b], Karima Megdouli [c], Ezzedine Nehdi [b]

[a] Mechanical Engineering Department, Jordan University of Science and Technology, Irbid, Jordan
[b] Laboratory Energetic & Environment, National Engineering School of Tunis, 37 Le Belvédère, Tunis, Tunisia
[c] Sorbonne Université, Institute Jean Le Rond D'Alembert, Faculté des Sciences et Ingénierie, Campus Pierre et Marie Curie, 75252, Paris Cedex 05, France

ABSTRACT

This study explores the integration of parallel compression and a two-phase ejector in transcritical CO_2 refrigeration systems, aiming to improve efficiency and performance. This innovative approach bridges the gap between conventional approaches and explores new energy-saving potential. The study uses thermodynamic modeling, mathematical simulation, and in-depth analysis to look at energy and exergy performance in a new configuration for applications in the retail sector at medium evaporation temperatures. The work investigates thermodynamic phenomena in a novel cycle with steady-state conditions, low pressure differentials, and adiabatic efficiency. The model is validated against experimental and theoretical published data, revealing component-specific exergy destruction and key parameters. The novel cycle efficiently extracts heat at higher temperatures, outperforming conventional and parallel cycles. Exergetic efficiency surpasses the standard cycle, with gas cooler pressure and temperature dependence enhancing efficiency by 40%–45%. The distribution of exergy destruction percentages reveals efficiency determinants, emphasizing heat exchange optimization and ejector responsiveness in energy dissipation dynamics. The study investigates the coefficient of performance (COP) dependence on gas cooler pressure and temperature, revealing superior performance compared to conventional cycles. COP increases by 50% at 80 bars, indicating enhanced efficiency. The new cycle offers exceptional efficiency gains, with a COP enhancement of over 75% for evaporator temperature transitions. Comparative analysis shows a COP superiority of up to 53% for lower evaporator temperatures and 20% for higher evaporator temperatures, demonstrating substantial energy savings and improved performance across various operating conditions.

1. Introduction

Forty percent of Europe's total electricity use goes toward heating and cooling. The refrigeration utilized by European retailers can have serious effects on the natural world. This is because many stores employ hydrofluorocarbon (HFC) based refrigerants in their refrigeration systems. When discharged into the atmosphere, these coolants have a high global warming potential (GWP) and

---

Nomenclature

A	Area [m^2]
COP	Coefficient of Performance [−]
$\dot{E}$	Exergy flow rate [kW]
e	Specific exergy [kJ/kg]
h	Specific enthalpy [kJ/kg]
$\dot{m}$	Mass flow rate [kg/s]
P	Pressure [bar]
$\dot{Q}$	Heat transfer rate [kW]
q	Vapor quality [−]
s	Specific entropy [kJ/kg-K]
T	Temperature [K]
u	Velocity [m/s]
$\dot{W}$	Power [kW]
MRE	Mean relative error [%]
MAE	Mean absolute error [−]

Greek Letters

η	Efficiency [%]
ρ	Density [kg/m^3]
φ	Ejector area ratio ($\frac{A_{mix}}{A_t}$) [−]
ψ	Exergy efficiency [%]
ω	Ejector entrainment ratio $\left(\frac{\dot{m}_s}{\dot{m}_p}\right)$ [−]

Superscripts & Subscripts

0	Reference
1,2,3 …	state points
b	back pressure
c	compressor
ch	chemical
d	exergy destruction
e	evaporator
ej	ejector
f	exergy fuel
gc	gas cooler
is	isentropic
kn	kinetic
mix	mixing chamber
n	nozzle
p	primary flow/exergy product
ph	physical
pt	potential
s	secondary flow
sa	after shock wave
sb	before shock wave
t	throat

---

exacerbate climate change. Furthermore, the energy used to run these refrigeration systems might contribute to global warming pollution. The use of more energy-efficient refrigeration systems and regular maintenance and servicing of current systems are two ways in which shops can lessen their negative effects on the environment [1]. Most heat pump systems use hydrofluorocarbons (HFCs) like R404A, R507A, and R134A, which have global warming potentials (GWPs) of 3922, 3985, and 1430, respectively. The European Union's "F-Gas" regulation, which seeks to combat global warming and reduce greenhouse gas emissions, prohibits the use of some HFCs due to their GPW. By 2030, the maximum GWP for authorized refrigerants in refrigeration systems will have dropped to 150. The regulation mandates the use of R744, which has a GWP of 1 and an ODP of 0, as a suitable substitute for the existing high GWP refrigerants. Additionally, the R744, which Lorentzen first presented in 1994 [2,3], is a safe alternative in terms of toxicity and flammability and is well-suited for refrigeration applications. The R744 is a step in the process of recycling carbon dioxide that can be recovered from other industrial processes to significantly lessen the greenhouse effect. The high thermal conductivity and high density of this refrigerant in the gas phase, in addition to its extreme environmental sensitivity, contribute to its excellent heat transfer in

evaporators, condensers, and gas coolers.

Due to its low critical temperature (31.1 °C) and high working pressures, which cause it to operate in transcritical conditions, the utilization of R744 does present some challenges. Transcritical systems have low efficiency and must attain a high compression ratio, which is a drawback. Since more steam must be created when the ambient temperature is high, this phenomenon is more significant. The COP of a refrigeration system using R744 has low energy performance for a condensation temperature close to the critical temperature, according to a comparison study of the COP of various refrigerants. Higher exergy losses during the gas cooling phase and the throttling, which are brought on by higher pressure decreases, are what account for this outcome [4].

The introduction of more complex cycles was necessary in order to attain commercially desirable performance and to be able to obtain operating efficiencies comparable to those of traditional refrigerants now in use. One of the proposed enhancements involved adding a subcooling system after the gas cooler. The R744 transcritical cycle, which uses a unique mechanical subcooling cycle, has been theoretically investigated [5] to see if it can improve the system's energy efficiency. Under the same operating conditions, the authors discovered a 20% improvement in the COP and a 28.8% improvement in the cooling capacity. The efficiency of the R744 transcritical cycle with specialized mechanical subcooling was examined [6]. A study was done on the energy and thermoeconomic of a R744 transcritical system that was cooled by a separate subcooling unit and used R1234yf as the coolant [7]. Their research's findings demonstrated that this suggested technique worked well even in hotter countries. The use of ejector and ORC was studied to utilize solar energy [8]. It has been suggested and investigated to use another R744 transcritical system with dedicated mechanical subcooling [9]. The system with dedicated mechanical subcooling decreased system operating pressure and increased COP by 61.76%, according to the data. According to the experimental findings on an R744 transcritical system with mechanical subcooling using R152a, there existed an ideal subcooling degree that was based on the temperatures of the evaporation and gas cooler for which the COP was highest [10].

Overfed evaporators, which are being investigated both theoretically and experimentally by a very large number of researchers, are another intriguing method of enhancing the R744 transcritical cycle in terms of cooling capacity and COP.

The redesigned supermarket refrigeration system with overfed evaporators and an accumulation tank was thoroughly examined in the middle and low temperature ranges [11]. For an outside temperature ranging from 10 to 40 °C, he discovered an improvement in the COP of between 4 and 21%. In a transcritical system with overfed evaporators, R744 performed better than R404a for ambient temperatures below 8 °C, according to a comparative analysis [12].

An energetic and thermo-economic analysis of the R744 transcritical system was investigated [13,14]. The models were resolved using REFPROP 10 in the MATLAB environment [15]. Economic and thermodynamic analyses were considered. When used in warm weather, the proposed technique produced superior outcomes. A study to find the supermarket's most effective configuration out of ten different configurations with and without overfed evaporators was conducted [16]. Theoretical results showed that the design with overfed evaporators, mechanical subcooling, and an intercooler may save 8.53 percent of annual power compared to the normal R404A system.

Eight distinct configurations of the R744 transcritical cycle with an overfed evaporator were examined [17]. Even in India's hottest regions, they were able to discover a new configuration whose energy performance was superior to that of the system using R404A. Multi-ejectors can be used to improve things even more. This concept's major goal is to minimize throttling losses. The R744 booster cycle with multiple ejectors was investigated, and various outcomes of the various configurations suggested were highlighted [18].

Parallel compression was also utilized in transcritical R744 refrigeration systems to improve efficiency. There has been study of this approach [19]. The outcomes demonstrated that the analyzed system's gas cooler's pressure was lower than that of the typical transcritical cycle. Parallel compression in the R744 transcritical refrigeration cycle was the subject of another theoretical investigation [20]. The COP increased by 47.3% with the suggested system. The transcritical R744 system's performance was assessed [21]. The experimental result was used to validate the numerically calculated results. Based on the results of experiments with the R744 transcritical system with parallel compression, these performances depended on the intermediate pressure, and there was a level for this pressure where the performances were at their best [22,23]. Additionally, this pressure is solely based on the evaporator's and the gas cooler's respective temperatures. Additionally, parallel compression was frequently used in booster systems for applications in supermarkets [24–26].

The R744 refrigerant has emerged as the refrigerant of the future because of recent extensive research and technology used to enhance the performance of transcritical cycles. There are more than 20,000 R744 transcritical refrigeration units in use today to cover up to 14% of all food installations in retail across Europe [27]. A comprehensive exergetic analysis of the transcritical vapor compression systems was conducted [28].

In the realm of refrigeration system research, a notable and intriguing gap exists, despite the abundance of research exploring the nuances of R744 installations and ways in which they could be improved. The prevailing focus has gravitated toward booster systems, marked by dual evaporators and compressors, inadvertently sidelining an unexplored realm ripe with innovation and simplicity. This study explores a parallel compression cycle that incorporates a two-phase ejector into the conventional transcritical cycle. Few works have studied this unexplored path of investigating the usual transcritical cycle under the auspices of parallel compression. Within the confines of the small transcritical cycle, this investigation sets out on an analytical quest to comprehend the broad set of energy and exergy performances created by the combination of parallel compression and a two-phase ejector. Particularly in the context of medium evaporation temperature applications, which is an important factor in the busy retail sector, the spotlight shines on the potential brilliance of this new combination. Intricately combining parallel compression with a two-phase ejector gives birth to a fresh idea that hasn't been explored before and is thus ripe for exploitation by the research community. Efforts will be focused on R744, a promising refrigerant that will change the face of retail refrigeration as transcritical installations become more commonplace. The potential radiant within this configuration is highlighted throughout the extensive research that follows; it has been specifically

designed to meet the medium evaporation temperature requirements of retail applications. Without a doubt, this cutting-edge CO_2 refrigeration system, enhanced by the synergistic abilities of an ejector and parallel compression, is the focus of energy, exergy, and exergoeconomic analysis. This study explores energy consumption reduction in the transcritical CO_2 refrigeration cycle, navigating diverse operational conditions and exploring variables, showcasing dedication to scientific inquiry. Illuminating the path to maximum performance, this paper takes the stage, weaving an intricate narrative of innovation, simplicity, and promise, destined to leave an indelible mark upon the annals of refrigeration system research. To demonstrate the advantages of the new cycle, a comparative analysis with both the conventional and parallel compression refrigeration cycles will be conducted.

2. System description

The significance of adopting CO_2 as a refrigerant is underscored by the stringent regulations imposed on high-GWP refrigerants. While CO_2 boasts an eco-friendly profile, its challenges lie in the juxtaposition of a low critical temperature and elevated operating pressure, inevitably culminating in heightened energy consumption, particularly evident within the realm of commercial refrigeration. Consequently, a surge in research endeavors and innovative enhancements is spurred forth. Fig. 1 shows that the refrigeration cycle starts when the refrigerant enters the ejector nozzle at point (4). It then speeds up to create a low-pressure suction zone in the suction region, where it pulls the two-phase refrigerant from point (10) in separator 2. These two flows converge, progressing through the diffuser, elevating the pressure, and culminating in the refrigerant's departure from the ejector at point (5), entering separator 1. Within separator 1, the liquid state (8) descends, traversing an expansion valve to reach separator 2, effecting pressure reduction at point (9). Simultaneously, vapor in state (6) from the separator is drawn into compressor 2, compressed to state (7) at a higher pressure. The liquid refrigerant at state (11) emanating from separator 2 undergoes expansion via an expansion valve, transitioning to state and pressure conditions suitable for the evaporator (state 12). Here, it enters as a two-phase liquid, enabling evaporation and the
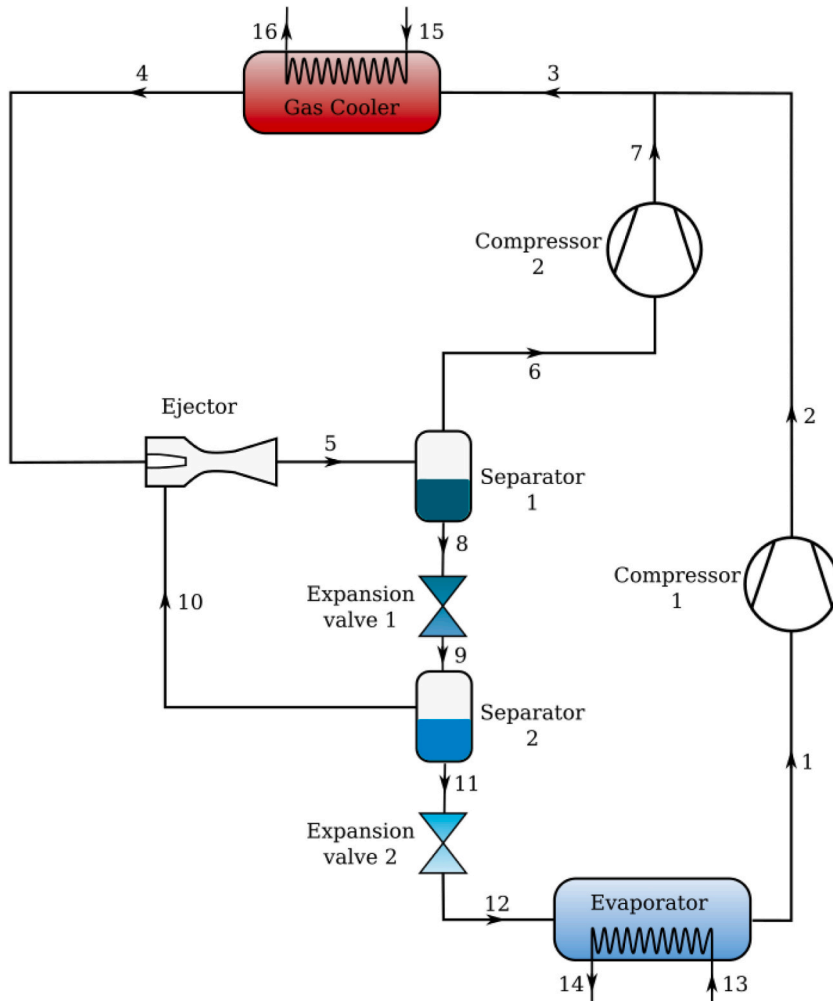

Fig. 1. Schematic of the new cycle.

generation of cooling capacity, $\dot{Q}_e$. Meanwhile, the saturated vapor at state (1) is inducted by compressor 1, pressurizing it to match the gas cooler pressure at state (2). The two high-pressure refrigerant streams converge at state (3) prior to entering the gas cooler, where the gas is condensed, releasing heat to the surroundings. The resulting liquid refrigerant at state (4) is then directed back to the ejector, completing the cycle. The T-s diagram is shown in Fig. 2. The traditional compression refrigeration cycle is shown in Fig. 3(a) and the parallel compression cycle in Fig. 3(b).

3. Thermodynamic and mathematical simulation model

Thermodynamic modeling and mathematical simulation presented in this article are based on a set of underlying assumptions essential for modeling the systems under investigation. These equations form the foundation for all calculations and employ subscripts, as shown in Fig. 1.

The study begins with the premise that all system elements are in a constant state. Second, it assumes an adiabatic and irreversible compression process. The process of isentropic throttling is also considered. In addition, the model presumes a thorough separation procedure, with the result being saturated vapor and liquid phases at the outputs. The gas cooler is the only component that transfers heat to and from the outside air; hence, pressure losses in the refrigeration system are disregarded. Since it is assumed that the ejector's flow is one dimensional, a one-dimensional model is used to evaluate the device's performance. The refrigerant velocities at the inlets and outlets are also assumed to be very low.

3.1. The system energy analysis

The equations describing the proposed simulation model are derived by applying the laws of energy conservation to each component in a steady-state regime. The following calculations are performed for each component:

Evaporator:

Evaporator capacity is calculated by Equation (1):

$$\dot{Q}_e = \dot{m}_1 \cdot (h_1 - h_{12}) \tag{1}$$

Compressor 1:

Under the assumption of isentropic compression, the outlet enthalpy $h_{2,is}$ is calculated as a function of P_2 and $s_{2,is}$, Equation (2):

$$s_{2,is} = s_1 \tag{2}$$

Then h_2 can be found with the following Equation (3):

$$h_2 = h_1 + \frac{(h_{2,is} - h_1)}{\eta_c} \tag{3}$$

Using Equation (4), the power consumption of compressor 1 is calculated as follows:

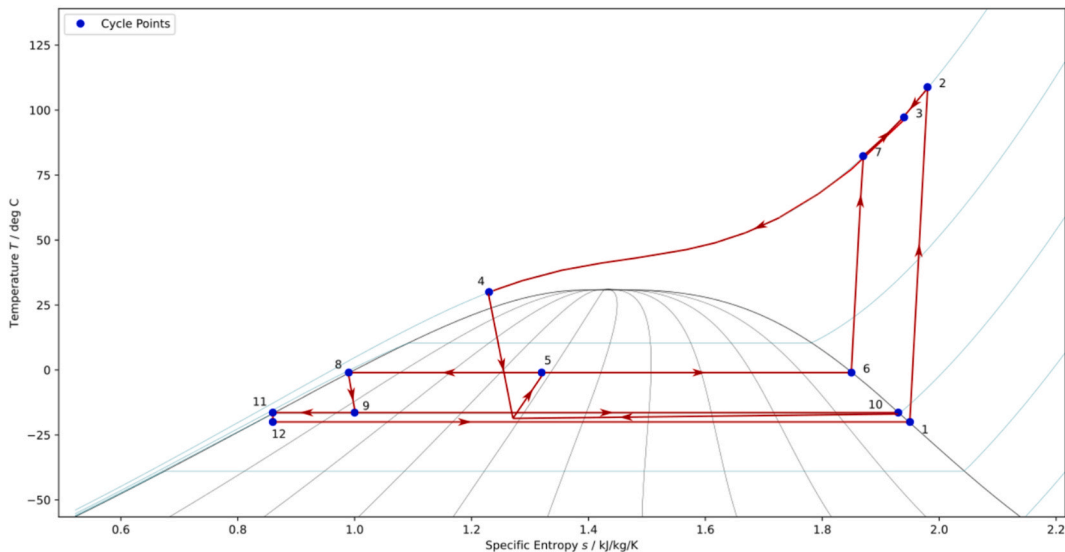$$\dot{W}_{c1} = \dot{m}_1 \cdot (h_2 - h_1) \tag{4}$$
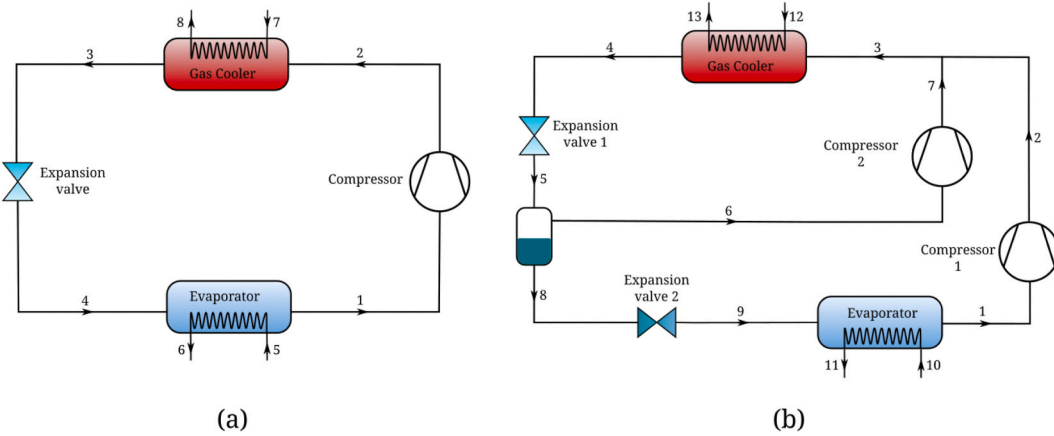

Fig. 2. T-s diagram.

Fig. 3. Schematic of the conventional compression refrigeration system (a), and the parallel cycle (b).

Compressor 2:

The same procedure as described in Equations (2)–(4) is repeated for compressor 2. The power consumption can then be calculated using Equation (5).

$$\dot{W}_{c2} = \dot{m}_6 \cdot (h_7 - h_6) \tag{5}$$

As shown in Equation (6), the mass flow at point 6 ($\dot{m}_6$) depends on the vapor quality at the ejector outlet (q_5):

$$\dot{m}_6 = \dot{m}_5 \cdot q_5 \tag{6}$$

Where $\dot{m}_5$ is found using the following Equation (7)

$$\dot{m}_5 = \dot{m}_4 + \dot{m}_{10} \tag{7}$$

The ejector calculation is done iteratively to find the pressure at point 9 (P9) that satisfies the given by Equation (8):

$$\omega_{ej} = \frac{(1 - q_5) \cdot q_9}{1 - (1 - q_5) \cdot q_9} \tag{8}$$

where ω_{ej} is the ejector entrainment ratio, calculated using the following Equation (9):

$$\omega_{ej} = \frac{\dot{m}_4}{\dot{m}_{10}} \tag{9}$$

as Equations (10) and (11) show, the expansion valves operate under an isenthalpic process:

$$h_8 = h_9 \tag{10}$$

$$h_{11} = h_{12} \tag{11}$$

The heat transfer in the gas cooler can be calculated using the following Equation (12):

$$\dot{Q}_{gc} = \dot{m}_3 \cdot (h_4 - h_3) \tag{12}$$

with:

$$h_3 = \frac{\dot{m}_2 * h_2 + \dot{m}_7 * h_7}{\dot{m}_3} \tag{13}$$

To calculate the COP, the following Equation (14) can be used:

$$COP = \frac{\dot{Q}_e}{\dot{W}_{c1} + \dot{W}_{c2}} \tag{14}$$

3.1.1. The ejector analysis

The ejector model is a one-dimensional, steady-state framework employed to anticipate the behavior of an ejector. It operates under specific assumptions:

Adiabatic flow, perfect mixing of primary and secondary flows, and negligible pressure drops across the mixing chamber.

This model relies on crucial input parameters for both primary and secondary flows, encompassing pressure (P_p, P_s), temperature

(T_p, T_s), mass flow rate $(\dot{m}_p)$, isentropic efficiencies $(\eta_n, \eta_s, \eta_y \text{ and } \eta_d)$, ejector area ratio (φ), and discharge pressure P_d. Central to the model are iterative calculations used to ascertain flow properties at various locations within the ejector. Assuming choked flow at the nozzle throat, flow properties are determined iteratively using the following Equations (15) and (16):

$$h_p = h_t + \frac{1}{2} * u_t^2 \tag{15}$$

$$\eta_n = \frac{h_p - h_t}{h_p - h_{t,is}} \tag{16}$$

This iterative process updates P_t until the difference between flow velocity, u_t, and the speed of sound (computed as a function of P_t, h_t, and q_t) falls within a predefined tolerance.

A similar procedure is applied to the secondary flow, assuming choking at a hypothetical throat in section Y. Equations (17) and (18) are used as follows:

$$h_s = h_{sy} + \frac{1}{2} * u_{sy}^2 \tag{17}$$

$$\eta_s = \frac{h_s - h_{sy}}{h_s - h_{s,is}} \tag{18}$$

With primary and secondary flows at pressure equilibrium at Y ($P_{py} = P_{sy} = P_y$), the primary flow velocity at section Y, u_{py}, is determined by Equation (19):

$$h_t + \frac{1}{2} * u_t^2 = h_{py} + \frac{1}{2} * u_{py}^2 \tag{19}$$

h_{py} is obtained through Equation (20):

$$\eta_y = \frac{h_t - h_{py}}{h_t - h_{py,is}} \tag{20}$$

The area occupied by the primary flow at Y is calculated as shown in Equation (21):

$$A_{py} = \frac{\dot{m}_p}{\rho_{py} * u_{py}} \tag{21}$$

subsequently, the area of the secondary flow at Y is using Equation (22):

$$A_{sy} = A_y - A_{py} \tag{22}$$

Where $A_y = A_t * \varphi$.

The following Equations (23) and (24) are used to calculate the ejector entrainment ratio (ω) and the secondary flow mass flow rate ($\dot{m}_s$), respectively:

$$\dot{m}_s = A_{sy} * \rho_{sy} * u_{sy} \tag{23}$$

$$\omega = \frac{\dot{m}_s}{\dot{m}_p} \tag{24}$$

Within the mixing chamber, flow properties are found iteratively by varying u_{mix}. Equations (25) and (26) govern this process as follows:

$$\dot{m}_p * \left(h_{py} + \frac{1}{2} * u_{py}^2 \right) + \dot{m}_s * \left(h_{sy} + \frac{1}{2} * u_{sy}^2 \right) = (\dot{m}_p + \dot{m}_s) * \left(h_{mix} + \frac{1}{2} * u_{mix}^2 \right) \tag{25}$$

$$u_{py} * \rho_{py} * A_{py} + u_{sy} * \rho_{sy} * A_{sy} = u_{mix} * \rho_{mix} * A_{mix} \tag{26}$$

If u_{mix} exceeds the speed of sound (calculated as a function of $P_{mix} = P_y$), h_{mix}, and q_{mix}, the flow undergoes a shock wave. In such cases, flow properties after the shock wave can be calculated using Equations (27)–(29), as follows:

$$(m_p + m_s) = \rho_{sa} * u_{sa} * A_{sa} \tag{27}$$

$$\frac{h_p + w * h_s}{1 + \omega} = \left(h_{sa} + \frac{1}{2} * u_{sa}^2 \right) \tag{28}$$

$$P_{sb} * A_{sb} + (m_p + m_s) * u_{sb} = P_{sa} * A_{sa} + (m_p + m_s) * u_{sa} \tag{29}$$

Finally, properties at the ejector's discharge are determined as functions of P_d and h_d, with h_d is found using the following Equation (30):

$$h_d = h_{sa} + \frac{1}{2} * u_{sa}^2 \tag{30}$$

3.2. The system exergy analysis

The "quality" of energy can be quantified using the thermodynamic notion of exergy. As a system approaches equilibrium with its environment, the maximum amount of work that can be taken from it is at its highest. As shown in Equation (31), there are four different kinds of exergy: physical, chemical, potential, and kinetic. The idea of exergy can be applied to better comprehend how effective energy systems are.

$$e_{tot} = e_{ph} + e_{kn} + e_{pt} + e_{ch} \tag{31}$$

in this analysis, the kinetic, potential, and chemical exergies of the working fluid are disregarded because there is no height change between components and no chemical reactions take place. Therefore, the total energy is equal to the physical energy, as shown in the following Equation (32):

$$e_{tot} = e_{ph} = (h - h_0) - T_0 * (s - s_0) \tag{32}$$

To which T_0, h_0, and s_0 refer to the reference temperature, enthalpy, and entropy, respectively. The values of T_0 and P_0, and hence h_0 and s_0, are dependent on the selected reference state.

Multiplying the mass flow rate, $\dot{m}$ by the exergy (e) yields the exergy flow rate for each stage of the cycle, as shown in Equation (33):

$$\dot{E} = \dot{m} * e \tag{33}$$

The exergy of the fuel ($\dot{E}_f$) and the exergy of the product ($\dot{E}_p$) are the two fundamental parameters used to calculate exergy destruction ($\dot{E}_d$) as shown in Equation (34):

$$\dot{E}_d = \dot{E}_f - \dot{E}_p \tag{34}$$

Table 1 provides a detailed examination of the exergy balance for all constituent parts.

4. Results and discussions

The discussion of the study's results is presented, and the transcritical refrigeration cycle paired with a two-phase ejector is discussed at length in this part. The mathematical models for the analyzed cycles were incorporated into a computer program developed using Python software. To determine the thermodynamic properties, we utilized the CoolProp library [29]. The flowchart of the simulation program is presented in Fig. 4.

The operating conditions and reference characteristics are set out in detail in Table 2 and serve as the basis for the analysis. Unless otherwise specified as variables, the following are the definitions of the characteristics required to generate the various results. It is recommended to keep the evaporator at $-30\ °C$, the gas cooler at $35\ °C$, the pressure at 9.5 MPa, and the ejector discharge at 4 MPa. These constants are used as starting points for the calculations.

The next step in the validation process involves comparing the collected results to data that has already been published, as shown in Table 3. There is a remarkable degree of consistency between the simulated results and the published data. This agreement provides strong support for the validity of the proposed model and the accuracy of the obtained simulations. These results lay the groundwork for a comprehensive discussion in which not only the intricacies of the proposed cycle are explained but also the enormous potential it has for transcritical refrigeration applications is shown.

Fig. 5 represents the validation of the parallel cycle model in comparison to experimental results from Chesi et al. [31]. The agreement of both data illustrates how the present model closely aligns with the real cycle's behavior. Nonetheless, distinctions do exist, mainly due to the simplifications that were made in this model. Notably, an assumption is made by setting the quality of the

Table 1
The balance exergy equations used in the analysis.

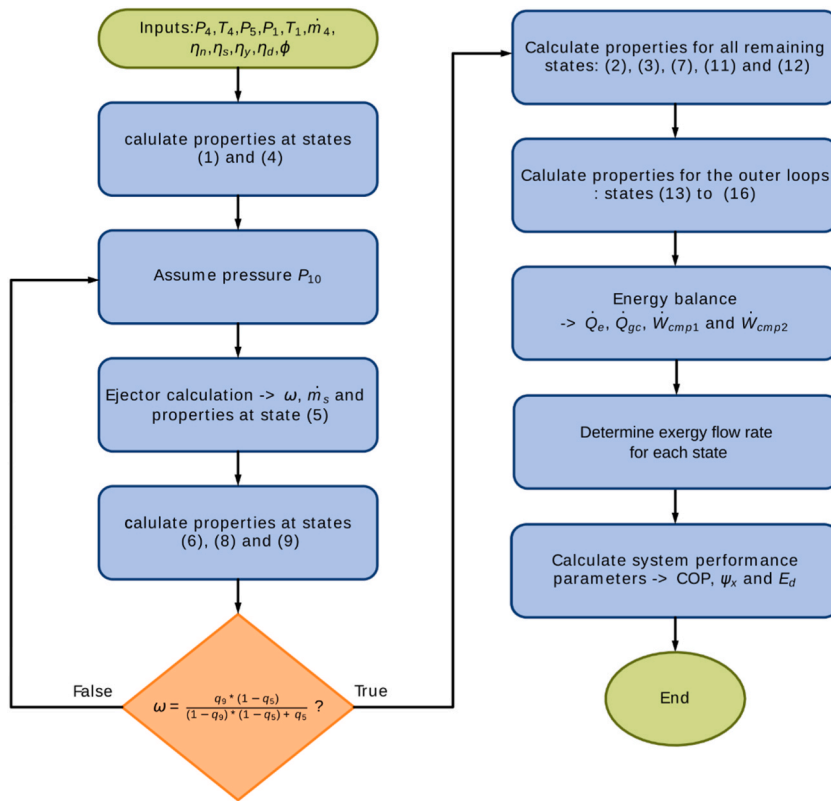| Component	Fuel	Product	Destruction
Compressor 1	$\dot{W}_{c1}$	$\dot{E}_2 - \dot{E}_1$	$\dot{W}_{c1} + \dot{E}_1 - \dot{E}_2$
Compressor 2	$\dot{W}_{c2}$	$\dot{E}_7 - \dot{E}_6$	$\dot{W}_{c1} + \dot{E}_1 - \dot{E}_3$
Gas cooler	$\dot{E}_3 - \dot{E}_4$	$\dot{E}_{16} - \dot{E}_{15}$	$\dot{E}_3 - \dot{E}_4 - \dot{E}_{16} + \dot{E}_{15}$
Ejector	$\dot{E}_4 + \dot{E}_{10}$	$\dot{E}_5$	$\dot{E}_4 + \dot{E}_{10} - \dot{E}_5$
Expansion valve 1	$\dot{E}_8$	$\dot{E}_9$	$\dot{E}_8 - \dot{E}_9$
Expansion valve 2	$\dot{E}_{11}$	$\dot{E}_{12}$	$\dot{E}_{11} - \dot{E}_{12}$
Evaporator	$\dot{E}_{12} - \dot{E}_1$	$\dot{E}_{14} - \dot{E}_{13}$	$\dot{E}_{12} - \dot{E}_1 - \dot{E}_{14} + \dot{E}_{13}$

Fig. 4. Flowchart of the simulation program.

Table 2
Operating conditions and reference parameters for the analysis of cycles performance.

Parameter	Value
Evaporator temperature	$-50\,°C$ to $-10\,°C$
Gas cooler temperature, T_{gc}	$25\,°C–40\,°C$
Gas cooler pressure	7.5 MPa–12 MPa
Compressors isentropic efficiency	0.75
Primary flow isentropic efficiency	0.93
Secondary flow isentropic efficiency	0.92
Diffuser isentropic efficiency	0.92
Temperature of reference state	$25\,°C$
Pressure of reference state	1 atm

liquid exiting the separator to 0 (pure liquid) in the present model. However, in the experimental work [31], the significance of the separator efficiency φ_{sep} was highlighted. This parameter is set to 0 when there is no separation in separator 2 and to 1 when the separation process is complete. The significance of this parameter on performance is highlighted by the observation that the COP of the cycle drops by a significant 9% when phi changes from 1 to 0.6.

Table 4 shows the thermodynamic properties at each state of the new cycle with working conditions as Te = $-30\,°C$, Tgc = $35\,°C$, P4 = 95 bar and P5 = 40 bar. The performance characteristics for the same working conditions are shown in Table 5.

The performance of the transcritical refrigeration cycle's components can be better understood due to the analyzing exergy destruction in the cycle. The percentages of exergy in the system's components are shown in Fig. 6. The results show that the exergy destruction across the cycle's core parts varies significantly under these conditions. Notably, the gas cooler (36.7%), compressor 1 (21.6%), and ejector (16.9%) account for most of the exergy destruction in the system. This indicates that improving the system's efficiency should focus on the gas cooler's performance and effectiveness. The evaporator plays a role in exergy degradation as well, though to a smaller level (only 9.5 percent). Exergy destruction is kept to a bare minimum using expansion valves 1 and 2, which account for 4.6% and 2.2%, respectively.

These findings highlight the need to improve transcritical refrigeration cycle efficiency and sustainability by enhancing heat exchange mechanisms like those in the gas cooler and evaporator. Efforts to boost the compressors' performance can also reduce exergy

Table 3
Validation of the ejector model with the work of Giacomelli et al. [30].

| N°	Pp [bar]	Tp [°C]	Ps [bar]	Ts [°C]	Pb [bar]	Wexp [−]	Wcalc [−]	Rerror [%]	Aerror [−]
1	37.89	36.9	30.83	10.5	37.89	0.194	0.201	3.383	0.007
2	36.72	36.6	24.87	12.6	36.72	0.098	0.114	14.298	0.016
3	37.29	36.4	28.4	10.8	37.29	0.163	0.181	10.055	0.018
4	37.71	35.5	32.76	9.7	37.71	0.242	0.226	−7.08	−0.016
5	35.84	36.6	24.65	13	35.84	0.102	0.122	16.148	0.02
6	37.16	35.8	32.13	10.2	37.16	0.24	0.231	−4.026	−0.009
7	36.57	35.9	29.45	9.6	36.57	0.196	0.195	−0.462	−0.001
8	36.83	36.2	34.78	10	36.83	0.296	0.294	−0.816	−0.002
9	36.19	35.8	27.1	13	36.19	0.154	0.158	2.215	0.004
10	41.38	37.3	37.9	10	41.38	0.412	0.463	11.015	0.051
11	40.21	37.7	29.29	13.6	40.21	0.241	0.196	−22.755	−0.045
12	40.79	37.5	33.82	9	40.79	0.33	0.359	8.189	0.029
13	41.05	37.2	35.94	10.2	41.05	0.374	0.416	10	0.042
14	41.34	36.9	38.59	9.7	41.34	0.431	0.48	10.208	0.049
15	38.69	37.4	24.17	13.8	38.69	0.135	0.123	−9.675	−0.012
16	39.51	37.5	26.43	13.9	39.51	0.182	0.135	−35.185	−0.047
17	40.34	37.4	31.14	8.3	40.34	0.277	0.266	−4.098	−0.011
18	42.22	36.9	38.62	9.9	42.22	0.433	0.47	7.936	0.037
19	42.16	36.9	39.39	9.6	42.16	0.45	0.49	8.245	0.04
20	39.28	34.9	30.13	11.5	39.28	0.255	0.218	−16.927	−0.037
21	37.54	34.6	23.9	13.3	37.54	0.133	0.109	−22.294	−0.024
22	38.49	33.9	27.34	12.9	38.49	0.21	0.155	−35.29	−0.055
23	37.9	33.8	25.21	12.7	37.9	0.165	0.114	−44.649	−0.051
24	40.02	33.2	35.27	10.3	40.02	0.372	0.329	−13.009	−0.043
25	39.7	35	32.19	8.6	39.7	0.358	0.325	−10.277	−0.033
26	40.43	35.5	31.13	22.2	40.43	0.338	0.24	−40.708	−0.098
MRE:		13.69 %							
MAE:		0.03							
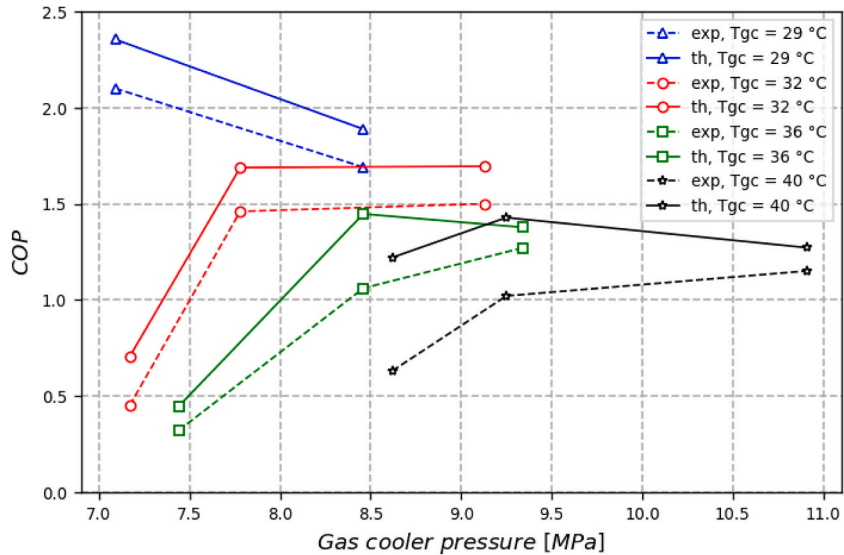
Fig. 5. Validation of the parallel compression cycle model with the experimental work of Chesi et al. [31].

destruction and increase cycle efficiency.

4.1. Parametric analysis

The investigation into the dependence of the COP on the gas cooler pressure and temperature yields intriguing findings that shed light on the system's thermodynamic behavior. As the gas cooler pressure experiences an augmentation, the COP exhibits a notable upward trend, indicative of enhanced system efficiency. However, this positive correlation reaches a point of diminishing returns beyond 85 bars, with subsequent pressure increases resulting in minimal COP improvement. This phenomenon signifies the emergence of a threshold where the COP plateaus, suggesting an asymptotic approach towards a constant COP value.

Table 4

New cycle thermodynamic properties.

State	Fluid	T [°C]	P [bar]	h [kJ.kg^{-1}]	s [kJ. (kg.K)$^{-1}$]	q [−]	m [kg.s^{-1}]	e [kJ.kg^{-1}]	E [kW]
1	CO_2	−30.00	14.28	436.82	2.00	1.000	0.51	151.27	77.7
2	CO_2	136.11	95.00	557.06	2.07	−	0.51	248.97	127.8
3	CO_2	104.93	95.00	515.32	1.97	−	1.00	238.88	238.9
4	CO_2	35.00	95.00	293.46	1.30	−	1.00	217.30	217.3
5	CO_2	5.30	40.00	307.29	1.38	0.439	1.11	204.87	226.9
6	CO_2	5.30	40.00	427.25	1.81	1.000	0.49	196.39	95.6
7	CO_2	77.19	95.00	471.27	1.85	−	0.49	230.97	112.4
8	CO_2	5.30	40.00	213.27	1.05	0	0.62	211.52	131.3
9	CO_2	−14.41	23.31	213.27	1.06	0.173	0.62	207.58	128.9
10	CO_2	−14.41	23.31	436.17	1.92	1.000	0.11	173.63	18.6
11	CO_2	−14.41	23.31	166.65	0.88	0	0.51	214.68	110.2
12	CO_2	−30.00	14.28	166.65	0.89	0.110	0.51	212.38	109.0
13	Air	−20.00	1.01	379.18	3.72	−	27.59	3.80	104.9
14	Air	−25.00	1.01	374.15	3.70	−	27.59	4.76	131.2
15	Air	25.00	1.01	424.44	3.88	−	44.09	0.00	0.0
16	Air	30.00	1.01	429.47	3.90	−	44.09	0.04	1.8

Table 5

New cycle energy performance characteristics.

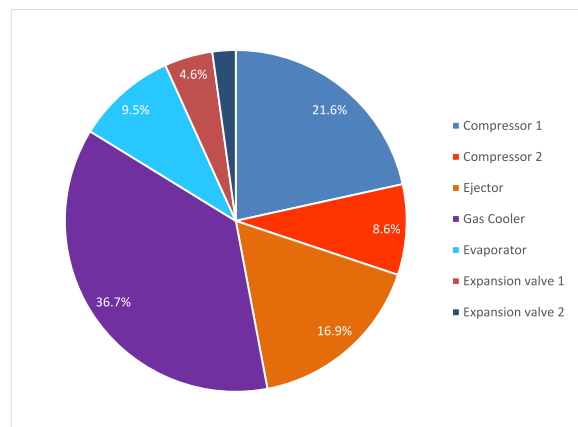|	
Cooling capacity $\dot{Q}_e$ [kW]	138.8
Gas cooler heat rejection $\dot{Q}_{gc}$ [kW]	223
Compressor 1 work $\dot{W}_{comp1}$ [kW]	63.3
Compressor 2 work $\dot{W}_{comp2}$ [kW]	20.85
Entrainment ratio ω [−]	0.095
Coefficient of performance COP [−]:	1.65
Exergy efficiency Ψx [%]:	33.2

Fig. 6. The overall exergy destruction attributed to each component and expressed as a percentage.

Remarkably, a substantial advancement in COP is observed at a pressure of 80 bars, boasting an impressive 44% and 8.9% increase compared to the conventional and parallel cycles, respectively. In contrast, the impact of T_{gc} on the COP exhibits a contrasting pattern. With a rise in T_{gc}, the COP exhibits a consistent decline. Notably, the COP value experiences a notable 45% reduction when the T_{gc} escalates from 25 to 45 °C. This inverse relationship between temperature and COP underscores the significance of carefully regulating T_{gc} to optimize system performance. To visually capture these intriguing trends, Figs. 7–10 depict the variation of COP in response to changes in P_4, T_{gc}, P_5 and T_e, respectively. This comprehensive representation provides a clear and insightful visualization of how system efficiency is influenced by these key parameters, offering valuable guidance for the design and operation of the refrigeration cycle.

The correlation between evaporator temperature and the COP, as shown in Fig. 10, is a crucial aspect that significantly impacts the performance of the refrigeration cycle. As the evaporator temperature increases, there is a discernible improvement in the COP. This relationship underscores the system's enhanced efficiency as it operates at higher evaporator temperatures. Notably, when considering a transition in evaporator temperature from −50 to −10 °C, the COP demonstrates a remarkable enhancement of over 98%. This
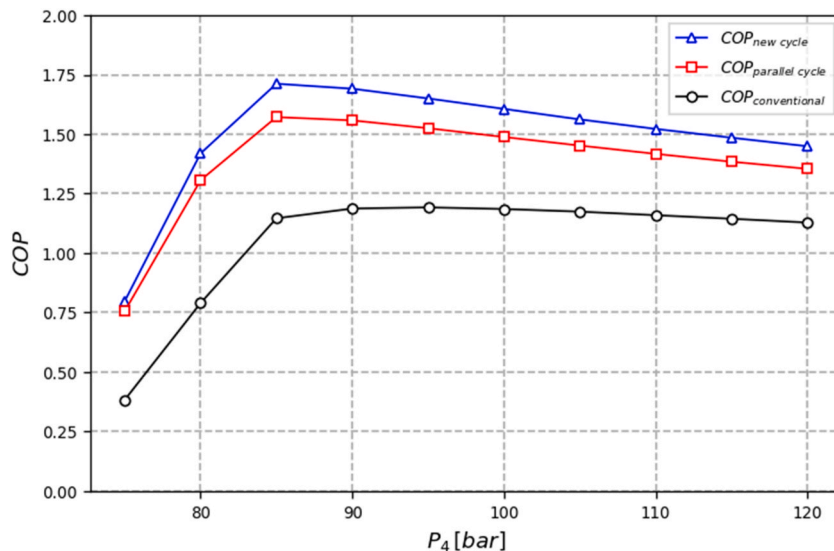
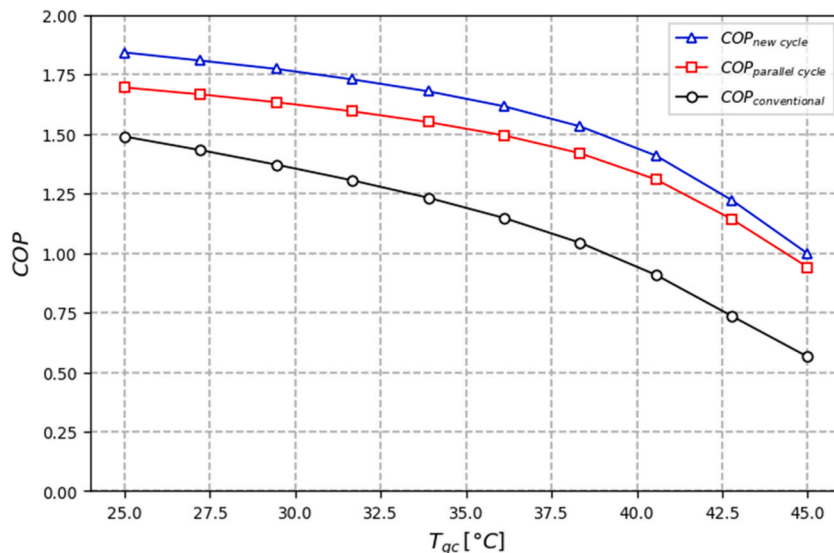**Fig. 7.** Variation of the COP vs the gas cooler pressure.

Fig. 8. Variation of the COP vs the gas cooler temperature.

substantial increase highlights the system's heightened capability to extract heat from the low-temperature reservoir and convert it into useful cooling. Moreover, the comparative analysis between the newly proposed cycle and the conventional cycle reveals compelling results. The novel cycle consistently outperforms its traditional counterpart by a notable margin, exhibiting a COP superiority of up to 53% for lower evaporator temperatures and up to 20% for higher evaporator temperatures. Also, in comparison to the parallel cycle, there was an increase by 11% for the lowest temperatures. As the evaporator temperature increases, the improvement in the COP decreases to 4.2% at -10 °C.

This research also investigated how different operating conditions affected the new cycle's, parallel, and conventional performance coefficients (COP_{new}, $COP_{parallel}$ and COP_{conv}), respectively. The results of the comparison demonstrated that, across the board, the new proposed cycle performed better than the alternative cycles. Compared to COP_{conv}, COP_{new} increased by an astounding 109 percentage points at a gas cooler pressure of 75 bars. In addition, it maintained a lead of over 6% over $COP_{parallel}$. At T_{gc} ranging from 25 °C to 45 °C, the new cycle demonstrated COP improvements of up to 24% and 77%, respectively, compared to COP_{conv}. The advantage over $COP_{parallel}$ was also consistent, with improvements exceeding 8% in all cases.

At the temperature extremes, ranging from -50 °C to -10 °C (T1), COP_{new} achieved significant improvements of up to 53% and 20%, respectively, compared to COP_{new}. It also showed a clear advantage over $COP_{parallel}$, with improvements ranging from 4% to 11%. Finally, regardless of varying ejector back pressures in bars, ranging from 30 to 50, COP_{new} consistently exceeded the values of
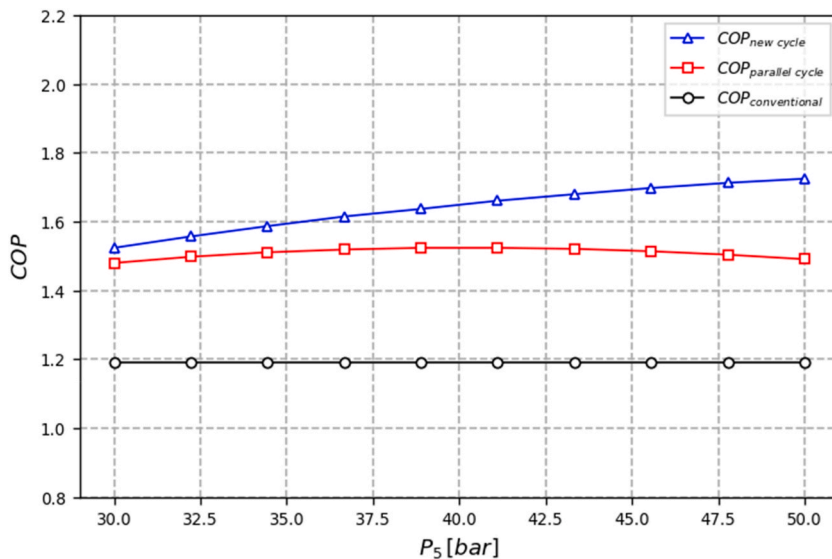
Fig. 9. Variation of the COP vs the compressor 2 inlet pressure.
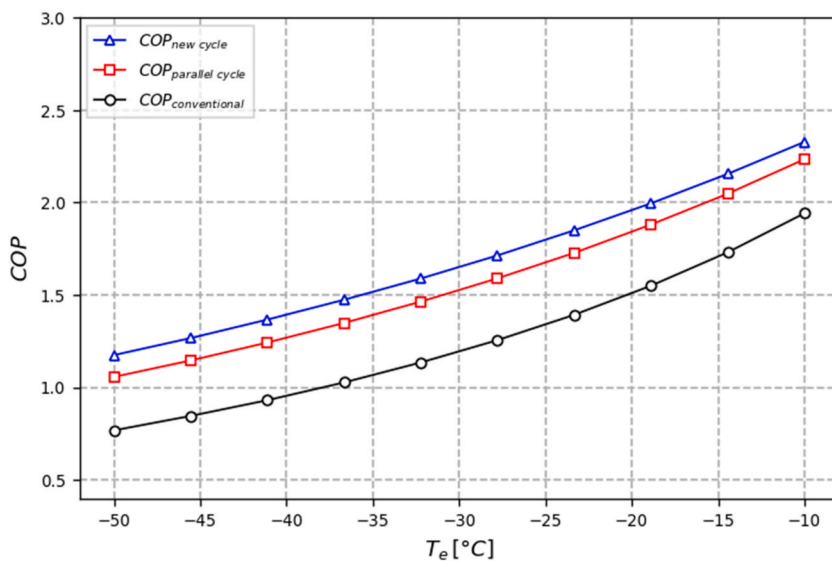

Fig. 10. Variation of the COP vs the evaporator temperature.

other cycles. The improvements ranged from 28% to 45% when compared to COP_{conv}. COP_{new} also maintained a significant advantage over $COP_{parallel}$, with improvements consistently exceeding 3% and reaching up to 16%. The results of this study suggest that the new cycle has the potential to be more efficient than the traditional and parallel cycles under a wide range of operating conditions.

This empirical evidence underscores the efficiency gains of the new cycle across a broad range of operating conditions, positioning it as a promising advancement in refrigeration technology with the potential to deliver substantial energy savings and improved overall performance.

The analysis of the proposed transcritical cycle yields compelling insights into its exergetic efficiency characteristics, as depicted in Figs. 11–14. Notably, as gas cooler pressure increases, exergetic efficiency demonstrates a consistent rise, culminating in its peak at an optimal pressure value of approximately 85 bars. Subsequent increments in gas cooler pressure beyond 90 bars yield marginal efficiency improvements, highlighting the system's sensitivity to pressure changes. Impressively, the new cycle's exergetic efficiency consistently outperforms the standard conventional cycle, exhibiting an average enhancement ranging from 40 to 45%. Conversely, the influence of T_{gc} on exergetic efficiency displays a diminishing pattern, with a significant 24% reduction observed as T_{gc} increases by 14°. A similar trend is observed with evaporator temperature, where a 40-degree elevation results in a 28% decrease in efficiency. Importantly, despite these fluctuations, the exergetic efficiency of the proposed cycle consistently surpasses that of the conventional
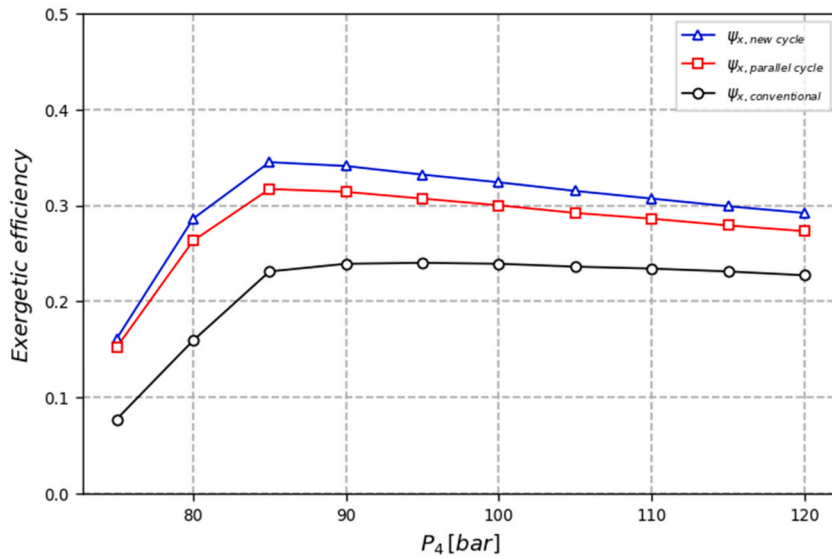
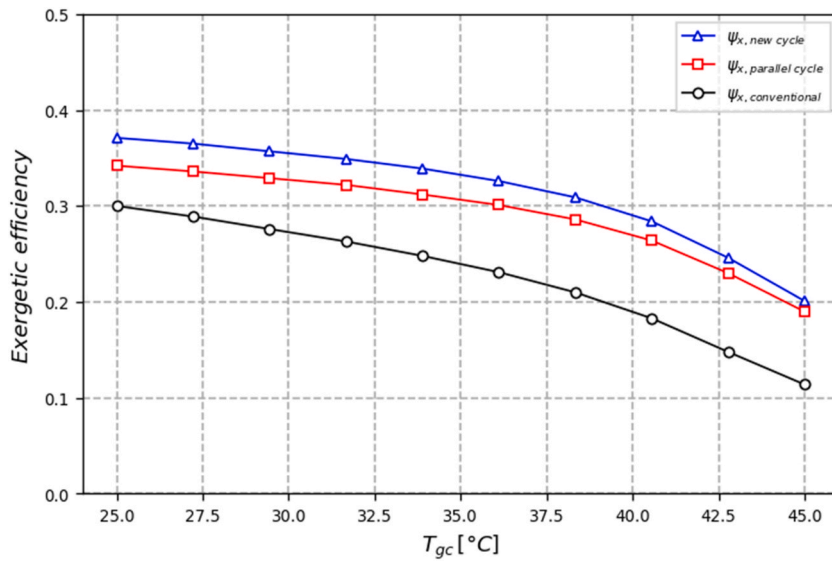**Fig. 11.** Variation of the exergy efficiency the gas cooler pressure.

Fig. 12. Variation of the exergy efficiency vs the gas cooler temperature.

transcritical cycle, underscoring its improved performance across a range of operating conditions.

These findings collectively reinforce the merits of the proposed transcritical cycle, positioning it as a promising advancement in energy-efficient refrigeration technology with its substantial exergetic efficiency gains and superior performance over the standard conventional cycle.

In this investigation, it has been noticed that the exergetic efficiency of the new cycle at different operating conditions consistently outperformed both the conventional and parallel cycles. At extreme temperature ranges (T1: $-10\,°C$ to $-50\,°C$), improvements ranged from 20% to 53% compared to the conventional cycle, and it maintained an advantage over the parallel cycle, with improvements of 4%–11%. For T_{gc} (25 °C–45 °C), the new cycle exhibited significant improvements, ranging from 24% to 76% compared to the conventional cycle, and similar enhancements were observed compared to the parallel cycle, exceeding 6% and reaching up to 9%. Regarding gas cooler pressures (P4: 75–120 bars), the new cycle achieved a remarkable 109% increase at 75 bars compared to the conventional cycle, consistently staying more than 6% ahead of the parallel cycle.

Under varying ejector back pressures (P5: 30–50 bars), the new cycle consistently outperformed the other cycles, with improvements ranging from 28% to an impressive 45% compared to the conventional cycle, and it also held an advantage over the parallel cycle, consistently exceeding 3% and reaching up to 16%. These findings emphasize the new cycle's consistent ability to enhance
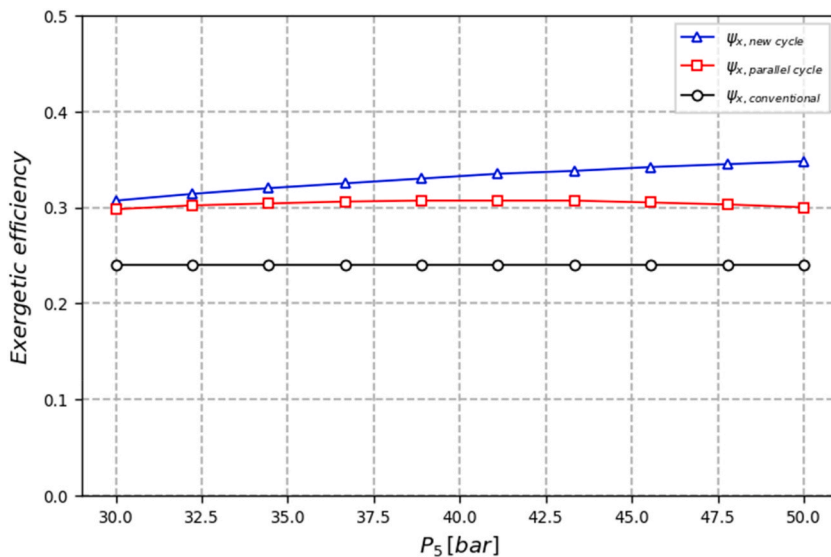
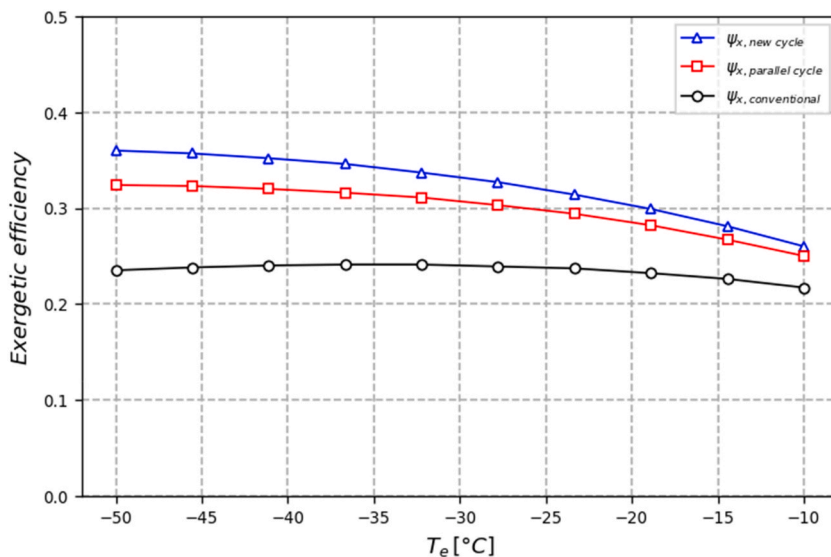**Fig. 13.** Variation of the exergy efficiency vs the compressor 2 inlet pressure.

Fig. 14. Variation of the exergy efficiency vs the evaporator temperature.

exergetic efficiency across diverse operating conditions, making it an excellent choice for optimizing energy utilization in cooling systems.

The investigation into the distribution of exergy destruction percentages across the system's components in response to variations in gas cooler pressure, as shown in Fig. 15, reveals intriguing trends. As gas cooler pressure escalates from 80 bars to 120 bars, a substantial increase of over 75% in exergy destruction percentage within the gas cooler is evident. The evaporator's contribution to exergy destruction exhibits the highest percentage up to 90 bars of gas cooler pressure, beyond which the gas cooler's share becomes dominant and continues to rise. Following a similar pattern, the ejector's contribution tracks the gas cooler and evaporator percentages, while the compressors and expansion valves consistently exhibit the lowest percentages of exergy destruction. Beyond the 90-bar threshold, gas cooler exergy destruction percentage maintains an upward trajectory, contrasting with the decreasing trends observed for the evaporator and ejector. Notably, exergy destruction percentages for the remaining components remain relatively constant across the pressure range. These findings underscore the intricate interplay between gas cooler pressure and component-specific exergy destruction percentages, shedding light on critical efficiency determinants within the refrigeration cycle. The exergy destruction percentages of each system component relative to the gas cooler pressure (P4) in bars exhibit several trends. The ejector's exergy destruction percentage decreases remarkably from 53.056% at 75 bars to 16.077% at 120 bars, suggesting that it becomes more
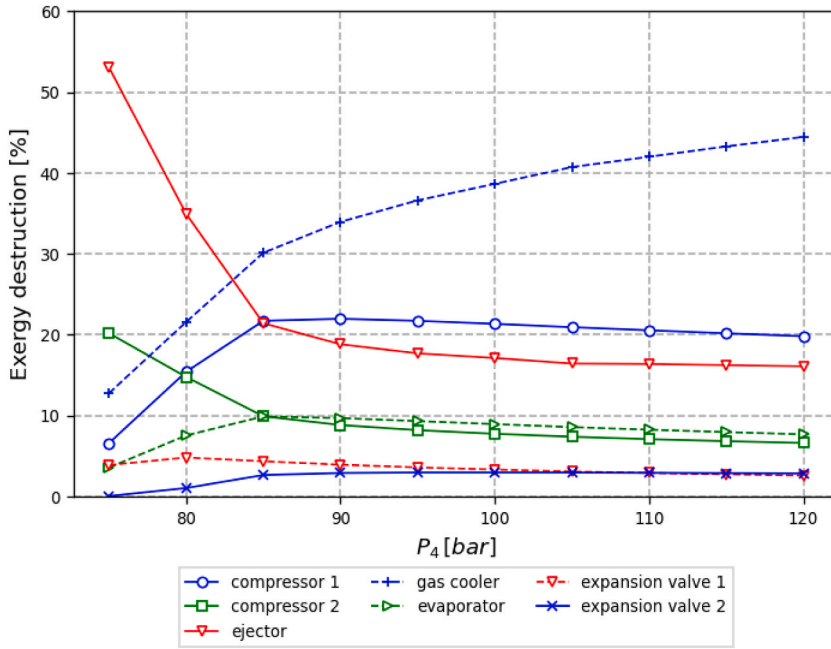
Fig. 15. Variation of the percentages of the components' contribution to the total amount of exergy destruction vs the gas cooler pressure.

efficient at higher pressures. The gas cooler's exergy destruction percentage steadily increases from 12.736% at 75 bars to 44.444% at 120 bars, indicating that it plays a progressively more substantial role in exergy losses as pressure levels rise. The second compressor's exergy destruction percentage consistently decreases from 20.176% at 75 bars to 6.598% at 120 bars, highlighting improved efficiency and reduced exergy losses at higher pressures. The first compressor's exergy destruction percentage increases from 6.575% at 75 bars to 19.808% at 120 bars. The evaporator's exergy destruction percentage slightly increases from 3.554% at 75 bars to 7.665% at 120 bars, suggesting that its efficiency improves to some extent at higher pressures. The gas cooler becomes a more significant contributor to exergy losses as pressure levels rise, while the ejector and second compressor become more efficient at higher pressures. The first compressor's exergy destruction increases with pressure, and the evaporator's efficiency improves to some extent at higher pressures.
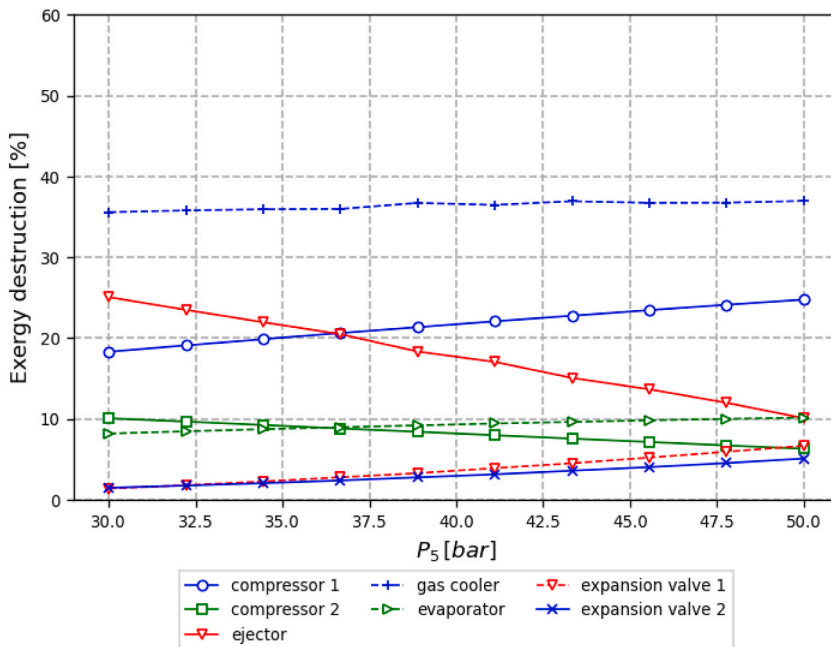

Fig. 16. Variation of the percentages of the components' contribution to the total amount of exergy destruction vs ejector discharge pressure.

The expansion valves contribute slightly to the overall exergy losses.

Fig. 16 displays the results of analyzing the exergy destruction inside the system as a function of the discharge pressure of the ejector. Exergy destruction was measured throughout a range of pressures from 30 to 50 bars, and it was found that the gas cooler consistently had the highest value, at around 37%. This finding hints at the possibility of significant gains for the whole system from enhancing the gas cooler's efficiency. In contrast, the ejector's contribution to exergy destruction decreased with increasing discharge pressure, falling from 26% at 30 bars to 10% at 50 bars. This suggests that better ejector performance is possible at higher pressures due to lower irreversible losses. It is important to optimize compressor operation in response to changing system circumstances, as the exergy destruction ascribed to Compressor 1 increased by almost 40% as ejector discharge pressure rose. Interestingly, across the whole range of ejector pressures, the exergy destruction values of the other system components remained reasonably consistent at less than 10%. These results highlight the value of pressure management in improving system effectiveness.

The exergy destruction percentages of each system component relative to the ejector back pressure (P5) in bars provide insights into their contributions. The gas cooler's exergy destruction remains relatively stable as ejector back pressure varies, ranging from 35.562% at 30 bars to 36.968% at 50 bars, indicating consistent performance regardless of changes in ejector back pressure. The ejector's exergy destruction, which initially has a significant impact, decreases with higher ejector back pressure, going from 25.053% at 30 bars to 10.079% at 50 bars. This suggests improved ejector efficiency at elevated back pressures. The first compressor's exergy destruction shows a slight increase as ejector back pressure rises, ranging from 18.296% to 24.755%. This indicates a decrease in efficiency and a larger contribution to exergy losses at higher ejector back pressures.

In contrast to the first compressor, the second compressor exhibits a decrease in exergy destruction with increasing ejector back pressure, with values ranging from 10.068% to 6.3%. This suggests enhanced efficiency and a lower role in exergy losses at higher back pressures. The evaporator's exergy destruction slightly rises as ejector back pressure increases, going from 8.176% to 10.15%. This indicates a modest reduction in the evaporator's efficiency under elevated ejector back pressures. Both expansion valves exhibit the smallest contributions to exergy destruction as ejector back pressure rises. The first expansion valve ranges from 1.377% to 6.666%, while the second one ranges from 1.47% to 5.081%.

The exploration of exergy destruction percentages across the system's components concerning variations in T_{gc} offers valuable insights into the cycle's performance. Fig. 17 shows that between 25 and 40 °C, both the gas cooler and the evaporator appear as major contributors to exergy destruction, with the gas cooler constantly retaining the largest proportion beyond the 40 percent level. Notably, as T_{gc} increases, a modest decline of 5% is observed in the exergy destruction percentages for both the evaporator and gas cooler. This subtle reduction suggests a slight shift in energy dissipation patterns as the system operates at higher T_{gc}.

Remarkably, the behavior of the ejector stands out prominently within the temperature spectrum. For T_{gc} below 35 °C, the rise in exergy destruction percentage attributed to the ejector remains marginal. However, an intriguing phenomenon unfolds as the temperature reaches 40 °C, with the ejector's percentage nearly doubling. This sharp increase emphasizes the heightened significance of ejector exergy destruction in scenarios of elevated T_{gc}.

Conversely, the remaining system components exhibit minimal fluctuations in exergy destruction percentages as the T_{gc} rises. Their consistently low contribution underscores their relative stability and minor influence on overall system efficiency. In light of these
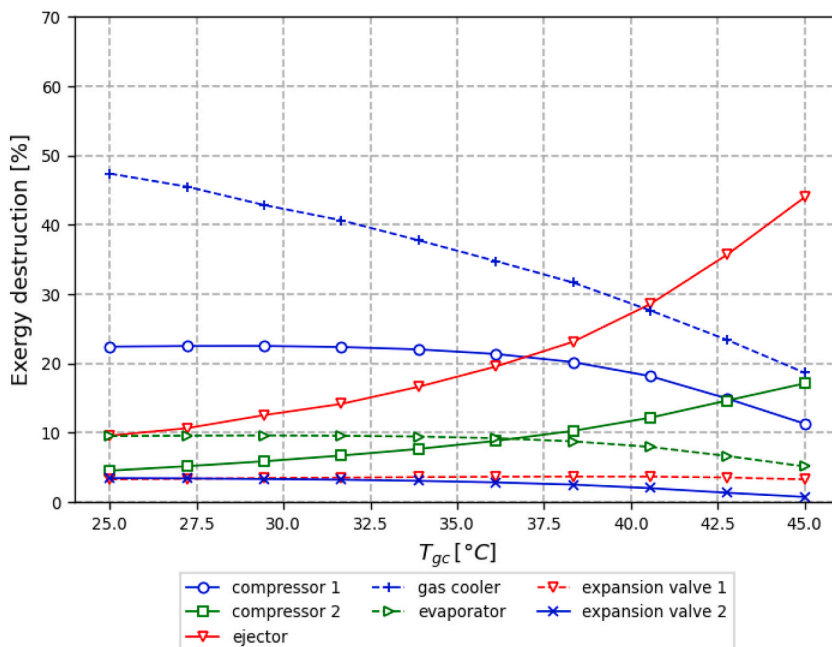

Fig. 17. Changes in the gas cooler's temperature and the percentages of the components' exergy destruction contributions.

findings, particular attention should be directed towards monitoring and optimizing the evaporator, gas cooler, and ejector components, especially when operating conditions entail T_{gc} above 35 °C. This comprehensive analysis enhances our understanding of the intricate relationship between T_{gc} and component-specific exergy destruction, guiding strategic decisions for improving the overall efficiency and performance of the refrigeration cycle.

The exergy destruction percentages of each system component relative to the temperature of the gas cooler (T4) in °C reveal the following insights. The gas cooler's exergy destruction consistently decreases as the temperature of the gas cooler rises, starting at 47.374% at 25 °C and dropping to 18.623% at 45 °C. This trend highlights the significant reduction in exergy losses in the gas cooler with increasing temperature. The ejector's exergy destruction, while notably lower than the gas cooler at lower temperatures, increases as T_{gc} increases, ranging from 9.543% at 25 °C to 43.957% at 45 °C. This suggests that the ejector becomes less efficient at higher temperatures. The first compressor's exergy destruction experiences a moderate decrease as T_{gc} changes, ranging from 22.4% at 25 °C to 11.268% at 45 °C. This suggests that the first compressor becomes more efficient at higher temperatures.

Contrary to the first compressor, the second compressor's exergy destruction undergoes a significant increase, with values ranging from 4.507% to 17.088%. This suggests that the second compressor becomes less efficient at higher temperatures. The evaporator's exergy destruction experiences a slight decrease as T_{gc} increases, going from 9.491% at 25 °C to 5.113% at 45 °C. This suggests that the evaporator becomes more efficient at higher T_{gc}. The exergy destruction in both expansion valves maintains stability with minor variations across different T_{gc}. They are the lowest contributors to the overall exergy losses.

In summary, the gas cooler becomes a less significant contributor to exergy losses as temperature levels rise, while the ejector and first compressor become more efficient at higher temperatures. The second compressor's exergy destruction increases with temperature, and the evaporator's efficiency improves to some extent at higher temperatures. The expansion valves contribute slightly to the overall exergy losses.

The comprehensive analysis of exergy destruction percentages across the various components concerning fluctuations in evaporator temperature, as illustrated in Fig. 18, provides valuable insights into the cycle's behavior. Notably, within the evaporator temperature range spanning from −50 to −35 °C, the evaporator emerges as the principal contributor to exergy destruction, accounting for the highest percentage at 45%. This emphasizes the pivotal role of the evaporator in energy dissipation within this temperature span.

Interestingly, as the evaporator temperature surpasses the −35-degree mark, a noteworthy shift in exergy destruction distribution unfolds. The exergy destruction percentage in the evaporator experiences a decline, coinciding with a concurrent increase in the gas cooler's contribution, which eventually peaks at 44% for an evaporator temperature of −10 °C. Thus, it becomes evident that the evaporator (29%) and the gas cooler (44%) jointly constitute the primary sources of exergy losses within the system. Meanwhile, the ejector's share of exergy destruction remains relatively moderate at 11% for an evaporator temperature of −10 °C, highlighting its intermediate role in energy dissipation.

Significantly, the behavior of the ejector demonstrates a notable sensitivity to changes in evaporator temperature. With the evaporator temperature's rise, the ejector's exergy destruction percentage experiences rapid escalation, further underscoring its responsive nature to shifting operating conditions. This intricate interplay between evaporator temperature and exergy destruction
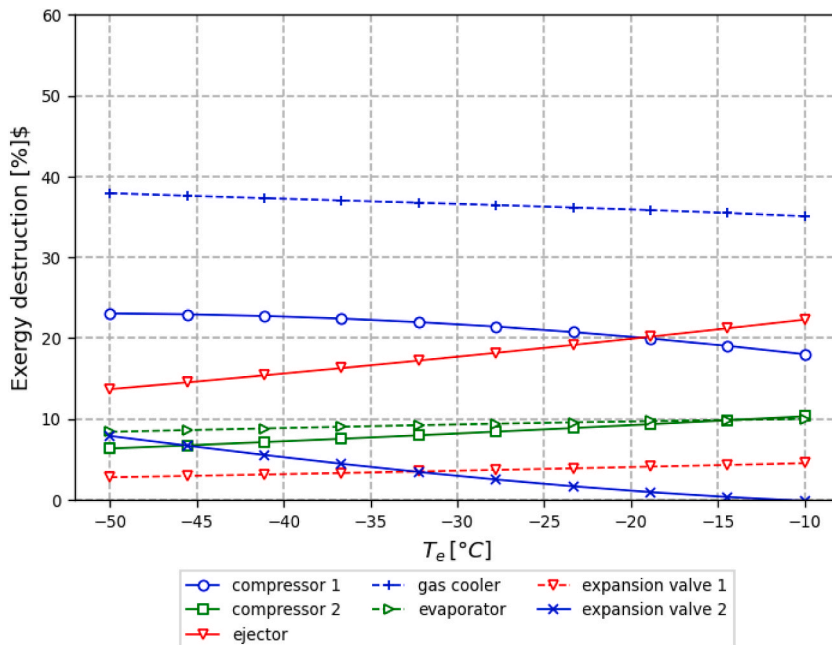

Fig. 18. Variation of the percentages of the components' contribution to the total amount of exergy destruction vs the evaporator temperature.

percentages across components unveils critical insights into the cycle's efficiency and performance dynamics. It underscores the importance of optimizing the evaporator and gas cooler while also shedding light on the significant influence of the ejector under varying evaporator temperature conditions. This knowledge guides informed decisions for system design and operation, ultimately contributing to enhanced energy efficiency and sustainable refrigeration practices.

The exergy destruction in the gas cooler consistently exhibits the highest exergy destruction, with percentages decreasing from 37.919% at $-50\,°C$ to 35.072% at $-10\,°C$. Following that, the first compressor contributes to exergy destruction, starting at 23.049% at $-50\,°C$ and decreasing to 17.986% at $-10\,°C$. Next in line is the ejector, which shows a continuous increase in exergy destruction, reaching 22.281% at $-10\,°C$. The evaporator follows with increasing destruction as temperature decreases, ranging from 8.384% to 9.987%. The second compressor exhibits exergy destruction, starting at 6.327% at $-50\,°C$ and increasing to 10.315% at $-10\,°C$. Finally, the two expansion valves contribute to a lesser extent to exergy destruction. This analysis underscores the dynamic interaction among these components as evaporator temperature varies, suggesting potential areas for system efficiency improvements, including gas cooler and ejector optimization.

5. Conclusions

This paper presents a novel transcritical refrigeration cycle configuration, integrating parallel compression and a two-phase ejector, enhancing energy and exergy performance, and contributing to refrigeration technology and system optimization. The proposed transcritical cycle outperformed the standard conventional cycle in terms of COP and exergetic efficiency, with average enhancements ranging from 40% to 45%. The study also highlighted the critical role of the gas cooler and evaporator in exergy destruction, emphasizing the need for heat exchange optimization. The study aims to comprehensively evaluate the energy and exergy performance of this innovative configuration, contributing valuable insights to refrigeration technology and system optimization.

The following key findings were noted:

- The investigated transcritical cycle consistently outperforms the conventional cycle, demonstrating average enhancements ranging from 40% to 45% in both the COP and exergetic efficiency.
- The substantial improvement underscores the potential for higher energy efficiency and sustainability in transcritical refrigeration applications.
- The study explores exergy destruction across cycle components, emphasizing the critical role of the gas cooler and evaporator in exergy destruction.
- The ejector's responsive behavior highlights the need for strategic optimization to minimize exergy destruction percentages under specific conditions.
- The new transcritical cycle consistently outperforms traditional and parallel cycles across a range of operational settings.
- Even at lower gas cooler pressures, the new cycle maintains a significant efficiency advantage over both conventional and parallel cycles.
- The new cycle's COP excels across a wide temperature range, demonstrating remarkable improvements, particularly at lower temperatures.
- At temperatures as low as $-50\,°C$, the new cycle consistently outperforms conventional and parallel cycles, showcasing its potential for diverse operating situations.
- In a refrigeration system, the gas cooler emerges as the primary contributor to exergy destruction, followed by the first compressor, ejector, and evaporator.
- Exergy destruction in the gas cooler decreases with increasing pressure and temperature, emphasizing the need for meticulous optimization of heat exchange processes.

Further recommendation

The study suggests studying the effect of increasing operating pressures and temperatures for both the gas cooler and ejector on the performance of the transcritical cycle. Also, It is recommended that expansion valves be investigated to evaluate how effective they could be in reducing exergy losses, which indicates potential areas for further optimization.

Data availability statement

No data was used for the research described in the article.

CRediT authorship contribution statement

Bourhan Tashtoush: Writing – review & editing, Supervision, Methodology, Formal analysis, Conceptualization. **Haythem Sahli:** Writing – original draft, Software, Methodology, Formal analysis, Data curation, Conceptualization. **Mouna Elakhdar:** Writing – original draft, Software, Project administration, Methodology, Investigation, Formal analysis, Conceptualization. **Karima Megdouli:** Writing – original draft, Validation, Software, Methodology, Investigation. **Ezzedine Nehdi:** Supervision, Resources, Project administration.

Declaration of competing interest

The authors declare that they have no known competing financial interests or personal relationships that could have appeared to influence the work reported in this paper.

References

[1] European Commission, Joint Research Centre, and European Technology Platform on Renewable Heating and Cooling (RHC-Platform), 2020–2030–2050, Common Vision for the Renewable Heating and Cooling Sector in Europe: European Technology Platform on Renewable Heating and Cooling, EUR-OP, Luxembourg, 2011.

[2] J.M. Belman-Flores, Vicente Pérez-García, Ituna-Yudonago, Jean Fulbert, Rodríguez-Muñoz, José Luis, Ramírez-Minguela, José de Jesús, General aspects of carbon dioxide as a refrigerant, J. Energy South Afr. 25 (2) (2014), 96-10.

[3] M.A. Islam, K. Srinivasan, K. Thu, B.B. Saha, Assessment of total equivalent warming impact (TEWI) of supermarket refrigeration systems, Int. J. Hydrogen Energy 42 (2017) 26973–26983.

[4] K. Megdouli, H. Sahli, B.M. Tashtoush, E. Nahdi, L. Kairouani, Theoretical research of the performance of a novel enhanced transcritical CO_2 refrigeration cycle for power and cold generation, Energy Convers. Manag. 201 (2019) 112139.

[5] Rodrigo Llopis, Ramón Cabello, Daniel Sánchez, Enrique Torrella, Energy improvements of CO2 transcritical refrigeration cycles using dedicated mechanical subcooling, Int. J. Refrig. 55 (2015) 129–141, https://doi.org/10.1016/j.ijrefrig.2015.03.016.

[6] P. Gullo, Advanced thermodynamic analysis of a transcritical R744 booster refrigerating unit with dedicated mechanical subcooling, Energies 11 (11) (2018) 3058, https://doi.org/10.3390/en11113058.

[7] G. Cortella, M.A. Coppola, P. D'Agaro, Sizing and control rules of dedicated mechanical subcooler in transcritical CO2 booster systems for commercial refrigeration, Appl. Therm. Eng. 193 (2021) 116953.

[8] Bourhan Tashtoush, Almutaz ballah R. Algharbawi, Parametric exergetic and energetic analysis of a novel modified organic rankine cycle with ejector, Therm. Sci. Eng. Prog. 19 (2020) 100644, https://doi.org/10.1016/j.tsep.2020.100644.

[9] Xi Liu, Kaihong Yu, Xinchen Wan, Xuelai Li, Performance evaluation of CO2 supermarket refrigeration system with multi-ejector and dedicated mechanical subcooling, Energy Rep. 7 (2021) 5214–5227.

[10] Laura Nebot-Andrés, Daniel Sánchez, Daniel Calleja-Anta, Ramón Cabello, Rodrigo Llopis, Experimental determination of the optimum intermediate and gas-cooler pressures of a commercial transcritical CO2 refrigeration plant with parallel compression, Appl. Therm. Eng. 189 (2021) 116671, https://doi.org/10.1016/j.applthermaleng.2021.116671.

[11] Nilesh Purohit, Vishaldeep Sharma, Samer Sawalha, Brian Fricke, Rodrigo Llopis, Mani Sankar Dasgupta, Integrated supermarket refrigeration for very high ambient temperature, Energy 165 (2018) 572–590, https://doi.org/10.1016/j.energy.2018.09.097. Part A.

[12] Vishaldeep Sharma, Brian Fricke, Pradeep Bansal, Comparative analysis of various CO2 configurations in supermarket refrigeration systems, Int. J. Refrig. 46 (2014) 86–99, https://doi.org/10.1016/j.ijrefrig.2014.07.001.

[13] Nilesh Purohit, Dileep Kumar Gupta, Mani Sankar Dasgupta, Energetic and economic analysis of trans-critical CO2 booster system for refrigeration in warm climatic condition, Int. J. Refrig. 80 (2017) 182–196, https://doi.org/10.1016/j.ijrefrig.2017.04.023.

[14] B. Peris Pérez, J.A. Expósito Carrillo, F.J. Sánchez de La Flor, J.M. Salmerón Lissén, A. Morillo Navarro, Thermoeconomic analysis of CO_2 ejector expansion refrigeration cycle (EERC) for low-temperature refrigeration in warm climates, Appl. Therm. Eng. 188 (2021) 116613.

[15] E. Lemmon, M. McLinden, M. Huber, NIST Standard Reference Database 23: Reference Fluid Thermodynamic and Transport Properties- REFPROP, Version 9.0, National Institute of Standards and Technology, Standard Reference Data Program, Gaithersburg, USA, 2010.

[16] Georgios Mitsopoulos, Evangelos Syngounas, Dimitrios Tsimpoukis, Evangelos Bellos, Christos Tzivanidis, Stavros Anagnostatos, Annual performance of a supermarket refrigeration system using different configurations with CO2 refrigerant, Energy Convers. Manag. X 1 (2019) 100006, https://doi.org/10.1016/j.ecmx.2019.100006.

[17] Manju Lata, Dileep Kumar Gupta, Performance evaluation and comparative analysis of trans-critical CO2 booster refrigeration systems with modified evaporative cooled gas cooler for supermarket application in Indian context, Int. J. Refrig. 120 (2020) 248–259, https://doi.org/10.1016/j.ijrefrig.2020.08.004.

[18] Parid Gullo, Impact and quantification of various individual thermodynamic improvements for transcritical R744 supermarket refrigeration systems based on advanced exergy analysis, Energy Convers. Manag. 229 (2021) 113684, https://doi.org/10.1016/j.enconman.2020.113684.

[19] S. Minetto, L. Cecchinato, M. Corradi, E. Fornasieri, C. Zilio, A. Schiavon, Theoretical and experimental analysis of a CO2 refrigerating cycle with two-stage throttling and suction of the flash vapour by an auxiliary compressor, in: IIR International Conference on Thermophysical Properties and Transfer Processes of Refrigerants, 2005. Vicenza (Italy).

[20] J. Sarkar, N. Agrawal, Performance optimization of transcritical CO2 cycle with parallel compression economization, Int. J. Therm. Sci. 49 (5) (2010) 838–843, https://doi.org/10.1016/j.ijthermalsci.2009.12.001.

[21] Andrea Chesi, Fabio Esposito, Giovanni Ferrara, Lorenzo Ferrari, Experimental analysis of R744 parallel compression cycle, Appl. Energy 135 (2014) 274–285, https://doi.org/10.1016/j.apenergy.2014.08.087.

[22] Laura Nebot-Andr', Daniel Calleja-Anta, Daniel S'anchez, Ram'on Cabello, Rodrigo Llopis, Experimental assessment of dedicated and integrated mechanical subcooling systems vs parallel compression in transcritical CO2 refrigeration plants, Energy Convers. Manag. 252 (2022) 115051.

[23] K.M. Tsamos, Y.T. Ge, I.D.M.C. Santosa, S.A. Tassou, Experimental investigation of gas cooler/condenser designs and effects on a CO2 booster system, Appl. Energy 186 (2017) 470–479.

[24] Xi Li, Kaihong Yu, Xinchen Wan, Xuelai Li, Performance evaluation of CO2 supermarket refrigeration system with multi-ejector and dedicated mechanical subcooling, Energy Rep. 7 (2021) 5214–5227, https://doi.org/10.1016/j.egyr.2021.08.110.

[25] Z. Sun, J. Li, Y. Liang, H. Sun, S. Liu, L. Yang, C. Wang, B. Dai, Performance assessment of CO 2 supermarket refrigeration system in different climate zones of China, Energy Convers. Manag. 208 (2020) 112572.

[26] Daniel Sacasas, Javier Vega, Cristian Cuevas, An annual energetic evaluation of booster and parallel refrigeration systems with R744 in food retail supermarkets. A Chilean perspective, Int. J. Refrig. 133 (2022) 326–336, https://doi.org/10.1016/j.ijrefrig.2021.10.010.

[27] Michal Haida, Michal Palacz, Jakub Bodys, Jacek Smolka, Paride Gullo, Andrzej J. Nowak, An experimental investigation of performance and instabilities of the R744 vapour compression rack equipped with a two-phase ejector based on short-term, long-term and unsteady operations, Appl. Therm. Eng. 185 (2021) 116353.

[28] B. Tashtoush, K. Megdouli, M. Elakhdar, E. Nehdi, L. Kairouani, A comprehensive energy and exergoeconomic analysis of a novel transcritical refrigeration cycle, Processes 8 (7) (2020) 758.

[29] I.H. Bell, J. Wronski, S. Quoilin, V. Lemort, Pure and pseudo-pure fluid thermophysical property evaluation and the open-source thermophysical property library CoolProp, Ind. Eng. Chem. Res. 53 (6) (2014) 2498–2508.

[30] F. Giacomelli, F. Mazzelli, K. Banasiak, A. Hafner, A. Milazzo, Experimental and computational analysis of a R744 flashing ejector, Int. J. Refrig. 107 (2019) 326–343.

[31] A. Chesi, F. Esposito, G. Ferrara, L. Ferrari, Experimental analysis of R744 parallel compression cycle, Appl. Energy 135 (2014) 274–285.